Integrated quantum well self-electro-optic effect device: 2×2 array of optically bistable switches

D. A. B. Miller and J. E. Henry
AT&T Bell Laboratories, Holmdel, New Jersey 07733

A. C. Gossard and J. H. English
AT&T Bell Laboratories, Murray Hill, New Jersey 07974

(Received 30 April 1986; accepted for publication 4 August 1986)

We demonstrate 2×2 arrays of optically bistable devices with very uniform optical characteristics. They are fabricated from an integrated self-electro-optic effect device structure consisting of a quantum well *p-i-n* diode grown in series with a load photodiode. Operating power can be optically controlled with a separate beam between ~40 pW and >470 μW with associated switching times of ~10 s and <2 μs.

One attractive feature of optics for switching and processing applications is its ability to communicate large amounts of information in parallel. To exploit this fully requires uniform, two-dimensional arrays of fast optical devices with low enough energy dissipation that their switching speed can be utilized in dense arrays without thermal problems. Some recent approaches use Fabry–Perot étalons containing semiconductor nonlinear refractive materials (see Ref. 1 for a general discussion) in which several different parts of the area of the étalon can be used simultaneously and independently.[2–4] Uniform operation over usable areas has been obtained.[3] Etching of mesas to overcome diffusion limits and shorten switching times has also been demonstrated.[4]

Another type of device, the quantum well self-electro-optic effect device (SEED),[5–9] relies first on the changes in optical absorption that can be induced by electric fields perpendicular to the thin semiconductor layers in quantum well materials, a mechanism called the quantum-confined Stark effect (QCSE).[10,11] Strong so-called "exciton" absorption resonances (e.g., ~10^4 cm^{-1} absorption coefficient) can be seen near the band-gap energy (e.g., at ~850 nm wavelength) at room temperature in quantum wells. The QCSE is an effect in which, among other things, these resonances can be moved spectrally with field. Combining the QCSE with optical detection within the same structure causes optoelectronic feedback that, when positive, gives optical bistability.[5–9] An optically bistable SEED generally consists of a diode containing quantum wells, an electrical load (e.g., a resistor), and, usually, a reverse bias voltage supply. The quantum well diode functions simultaneously as an absorption modulator and a detector. The wavelength is chosen so that the absorption (and hence the photocurrent) increases with decreasing reverse bias voltage on the diode; this behavior is seen near to the zero-field wavelength of the so-called "heavy-hole" exciton resonance. Hence increasing incident light gives increasing photocurrent that in turn results in reduced voltage on the diode because of the voltage drop across the resistor. Consequently the absorption and photocurrent increase, giving a positive feedback that can lead to switching into a high absorption state.

Other device functions are also possible.[6–9] The SEED does not require Fabry–Perot resonators. Consequently neither optical thickness nor operating wavelength is very critical. Because of the strength of the QCSE, SEED's also have the potential for very low total switching energy densities,[5,7] despite the absence of resonators to reduce switching energy.

The capacitances of the diode and the load, and any stray capacitances (except those across the power supply) must be charged or discharged for switching. Although internal capacitance could be made small in a small integrated structure, devices demonstrated to date have used external electrical components for the load, and there is little prospect of constructing such a circuit without ~1 pF capacitance. Arrays also require separate loads for each device. In this letter, we describe a method for making arrays of SEED's with an integrated load that has the potential for overcoming these problems, and we present results for 2×2 SEED arrays. The structure used also has an optically controllable load that adds flexibility to the device.

The integrated SEED structure used here consists of a *p-i-n* diode with quantum wells in the intrinsic (*i*) region, vertically integrated in series with *another* photodiode (also a *p-i-n* structure) that is used instead of a resistor as the load.[7] This load photodiode is transparent to the infrared wavelengths used for the quantum wells, but is essentially opaque for all wavelengths <750 nm. In operation, a second short-wavelength control light beam (e.g., from a HeNe laser) is shone on this photodiode. The single device is shown schematically in Fig. 1, together with its equivalent circuit. Crudely speaking, this load photodiode can be regarded as a transparent resistor whose value can be externally set with another light beam. The operation of this device is therefore qualitatively similar to that of the resistor-loaded device. In actual fact, the load photodiode behaves more like a constant current load, and this kind of load can give better bistability compared to the resistor load.[7] The speed of switching is then set by the time taken for the difference in photocurrents in the two diodes to charge their capacitance rather than by a resistor-capacitor time constant. Switching occurs when the photocurrents in the load diode and in the quantum well diode are comparable. The control light power therefore sets the switching power and speed of the devices. The detailed behavior can be quantitatively understood by the use of load lines.[7]

 0003-6951/86/390821-03$01.00

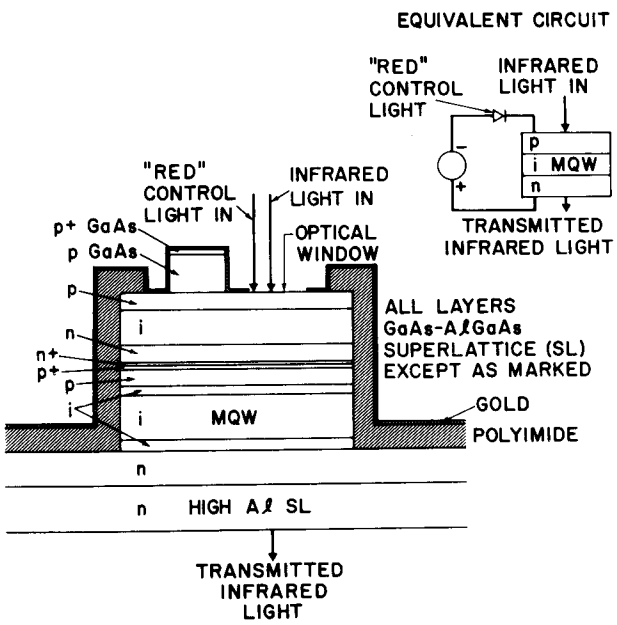

FIG. 1. Schematic diagram of the integrated SEED structure for a single device in an array, showing also the equivalent electrical circuit.

The structures are grown by molecular beam epitaxy starting with silicon-doped n-GaAs substrates. The sequence of regions is detailed in Fig. 1, and Tables I and II. We chose superlattice material of very fine period alternate layers of GaAs and AlGaAs in the structure rather than thick layers of AlGaAs because the use of superlattice may improve the quality of the material,[12] and because the average aluminum content of the layers can be adjusted without adjusting the temperature of the aluminum oven. Such fine superlattices behave approximately like the average alloy.

The first, high Al region is a stop layer for the substrate selective etch. In the quantum well p-i-n diode, in sample 1 only we included intrinsic buffer layers around the quantum well region as used previously (see, e.g., Ref. 11). The highly

TABLE I. Layer structure of samples.

Region	Total thickness (μm) Sample 1	Sample 2
Top contact		
p^+-GaAs	0.091	0.103
p-GaAs	0.820	0.923
Load diode		
p-SL	0.369	0.424
i-SL	0.738	0.847
n-SL	0.369	0.424
Tunnel junction		
n^+-SL	0.074	0.085
p^+-SL	0.074	0.085
Quantum well diode		
p-SL	0.369	0.424
i-buffer SL	0.183	...
i-quantum wells	0.976	1.537
i-buffer SL	0.183	...
n-SL	0.738	0.847
Etch stop		
n-high Al SL	0.932	1.103

TABLE II. Quantum well and superlattice material parameters.

	Sample 1	Sample 2
Al fraction in AlGaAs	0.297	0.345
Superlattice (SL)	18.4 Å GaAs	20.5 Å GaAs
	11.1 Å AlGaAs	13.4 Å AlGaAs
High Al SL	9.2 Å GaAs	10.3 Å GaAs
	84.0 Å AlGaAs	100 Å AlGaAs
Quantum wells	86.5 Å GaAs	92.4 Å GaAs
	51.0 Å AlGaAs	61.3 Å AlGaAs
Doping (10^{18} cm^{-3})		
p^+	10	10
p	1	1
n^+	3	3
n	1	1

doped tunnel junction grown next effectively makes an ohmic contact between the two p-i-n diodes, converting holes to electrons and inhibiting minority-carrier diffusion, a technique employed in stacking solar cells.[13–15] Next, the load p-i-n diode is grown. Finally, GaAs contact layers are grown. The thick layer spaces the contact from the diode junction to minimize dopant spiking. The highly doped layer facilitates good contacts.

To fabricate the devices, we first form the gold contacts for the top of the mesas by conventional photolithography and evaporation followed by thermal alloying of the contacts. This leaves a two-dimensional array of contacts, each $120\times50\,\mu$m, spaced on $400\,\mu$m centers. The GaAs top layer is removed everywhere else by masking and selective etching. Using further masking and etching, mesas approximately $200\,\mu$m square, also on $400\,\mu$m centers, are etched to a carefully controlled depth, so that the etching stops just within the bottom n-doped layers of the structure. The contacts lie toward one side of each mesa as shown in Fig. 1. Then an insulating layer of polyimide is spin deposited on the surface, and it is photolithographically patterned and etched by reactive ion etching to leave cleared squares on top of the desired mesas (see Fig. 1). Gold is then deposited on the top surface to connect all the contact regions, with $120\times50\,\mu$m rectangular optical windows being defined photolithographically and subsequently cleared by a lift-off step. The material is then cleaved to give separate 2×2 arrays of devices. A wire is epoxied to the top gold surface of an array, the array is stuck top down to sapphire with transparent epoxy, and the substrate is removed below the mesas of interest with a selective etch. Another contact wire is taken off the remaining substrate. This fabrication leaves a 2×2 array of devices with common top and bottom contacts but otherwise insulated. Finally, a silicon oxide antireflection coating is deposited on this exposed layer. We made several 2×2 arrays from each sample, with similar performance from all arrays from a given sample.

In operation, a voltage supply reverse biases the array through the two wires, and the light beams are incident on the mesa side of the devices (although the infrared light can be shone from either direction). We used a Styryl 9 dye laser for the infrared source for most experiments, although the devices were also tested using a commercial cw GaAs diode

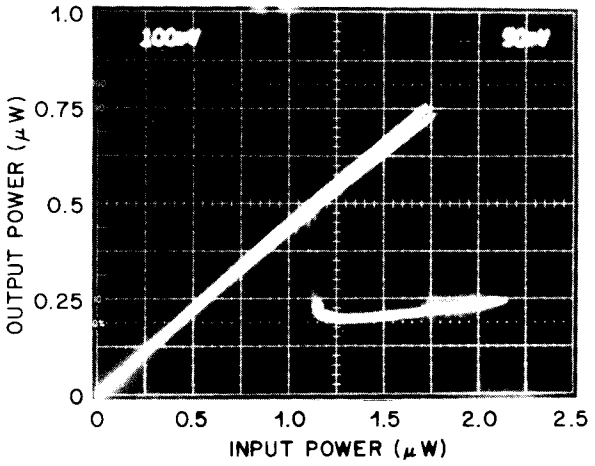

FIG. 2. Input/output characteristics for the four devices in an array superimposed. Sample 2. HeNe control power 1.95 μW (at 632.8 nm). Dye laser wavelength 857 nm. Supply voltage 28 V.

laser. HeNe and infrared beams were focused on the same mesa (they need not be coincident) using a 25 mm focal length lens, with a spot diameter of $\sim 20\,\mu$m. Powers were measured with Si photodiodes. To test for bistability, the infrared power was ramped up and down using an acousto-optic modulator. A typical input/output characteristic for the infrared beam is shown in Fig. 2. This picture shows the characteristics for the *four devices in an array superimposed.*

By varying the HeNe control beam power, we were able to vary the switching power and (reciprocally) the switching speed over a very large range. (By switching power we mean the total infrared input power at the point where the output power switches from high to low transmission). With sample 1 (sample 2) we observed bistability with switching powers as low as ~ 40 pW (~ 80 pW) and switching time of ~ 10 s (~ 15 s) at ~ 40 pW (~ 100 pW) HeNe control power; slightly lower power switching may be possible. At the high power extreme, we observed bistability up to a switching power of 6.1 μW (470 μW) at 100 μs (2 μs) with 6.3 μW (610 μW) HeNe power; for higher powers, the bistable loop progressively narrowed and disappeared. Bistability could be observed between 834 and 859 nm (846 and 869 nm), for voltages greater than 4 V (9 V). The optimum wavelength for large contrast ratio between the transmission in the two states was ~ 851 nm (857 nm), with ratios of 2.8:1 (3.5:1) obtained over a range of ~ 2 nm in both cases, at operating voltages of 25 V (28 V). The transmission in the high-transmission state under these conditions is $\sim 53\%$ (40%). Lower operating voltages gave smaller contrast ratio.

The lower limit on switching power will probably be set by leakage current, which we measure to be < 20 pA for the whole array. We believe that the upper limit on switching speed is set by the limited forward tunneling current of the tunnel junctions. Preliminary data on samples with improved tunnel junctions show switching speeds less than 1 μs, currently limited by laser power. The switching time at a given power is consistent with charging the device capacitance (~ 9 pF) to the supply voltage with the photocurrent.

In conclusion, we have demonstrated integrated arrays of SEED's with excellent uniformity of bistable switching characteristics. Optical control allows bistability over nearly seven orders of magnitude in switching power and speed. We expect that these devices can be scaled to much smaller lateral dimensions, with proportionate reduction in switching power, and possibly to larger arrays. More generally, this device demonstrates the real potential for sophisticated and novel optoelectronic devices operating under practical and flexible conditions using quantum well technology.

[1] H. M. Gibbs, *Optical Bistability: Controlling Light with Light* (Academic, New York, 1985).
[2] See, for example, D. J. Hagan, H. A. MacKenzie, H. A. Al Attar, and W. J. Firth, Opt. Lett. **10**, 187 (1985); D. J. Hagan, I. Galbraith, H. A. MacKenzie, W. J. Firth, A. C. Walker, J. Young, and S. D. Smith, in *Optical Bistability III*, edited by H. M. Gibbs, P. Mandel, N. Peyghambarian, and S. D. Smith (Springer, Berlin, 1986), p. 189.
[3] J. L. Jewell, Y. H. Lee, J. F. Duffy, A. C. Gossard, and W. Wiegmann, Appl. Phys. Lett. **48**, 1342 (1986).
[4] T. Venkatesan, B. Wilkens, Y. H. Lee, M. Warren, G. Olbright, N. Peyghambarian, J. S. Smith, and A. Yariv, Appl. Phys. Lett. **48**, 145 (1986).
[5] D. A. B. Miller, D. S. Chemla, T. C. Damen, A. C. Gossard, W. Wiegmann, T. H. Wood, and C. A. Burrus, Appl. Phys. Lett. **45**, 13 (1984).
[6] D. A. B. Miller, D. S. Chemla, T. C. Damen, T. H. Wood, C. A. Burrus, A. C. Gossard, and W. Wiegmann, Opt. Lett. **9**, 567 (1984).
[7] D. A. B. Miller, D. S. Chemla, T. C. Damen, T. H. Wood, C. A. Burrus, A. C. Gossard, and W. Wiegmann, IEEE J. Quantum Electron. **QE-21**, 1462 (1985).
[8] J. S. Weiner, D. A. B. Miller, D. S. Chemla, T. C. Damen, C. A. Burrus, T. H. Wood, A. C. Gossard, and W. Wiegmann, Appl. Phys. Lett. **47**, 1148 (1985).
[9] D. A. B. Miller, J. S. Wiener, and D. S. Chemla, IEEE J. Quantum Electron. **QE-22**, 1816 (1986).
[10] D. A. B. Miller, D. S. Chemla, T. C. Damen, A. C. Gossard, W. Wiegmann, T. H. Wood, and C. A. Burrus, Phys. Rev. Lett. **53**, 2173 (1984).
[11] D. A. B. Miller, D. S. Chemla, T. C. Damen, A. C. Gossard, W. Wiegmann, T. H. Wood, and C. A. Burrus, Phys. Rev. B **32**, 1043 (1985).
[12] P. M. Petroff, R. C. Miller, A. C. Gossard, and W. Wiegmann, Appl. Phys. Lett. **44**, 217 (1984); H. Morkoç in *Technology and Physics of Molecular Epitaxy*, edited by E. H. C. Parker (Plenum, New York, 1985), Chap. 7, p. 213.
[13] M. Ilegems, B. Schwartz, L. A. Koszi, and R. C. Miller, Appl. Phys. Lett. **33**, 629 (1978).
[14] P. Bouchaib, H. P. Contour, F. Raymond, C. Verie, and F. Arnaud D'Avitaya, J. Vac. Sci. Technol. **19**, 145 (1981).
[15] D. L. Miller, S. W. Zehr, and J. S. Harris, J. Appl. Phys. **53**, 744 (1982).